DOI: 10.61782/fa.2025.0464

FORUM ACUSTICUM
EURONOISE 2025

INCREASING HELMHOLTZ RESONATOR STABILITY AGAINST NON-LINEAR RESISTANCE INCREMENTS USING CHAMFERS

David Jun[1*] **Josef Plasek**[1] **Monika Rychtarikova**[2]
Zuzana Fisarova[1] **Christ Glorieux**[3]
[1] Brno University of Technology, Faculty of Civil Engineering, Brno, Czech Republic
[2] KU Leuven, Department of Architecture, Campus Brussels and Ghent, Brussels, Belgium
[3] KU Leuven, Department of Physics and Astronomy, Leuven, Belgium

ABSTRACT

Weakly damped Helmholtz resonators (WDHRs) are resonant devices with their surface resistance near resonance being substantially lower than the one of air and therefore the sound reflection at their resonance is out-of-phase. They are known for their absorption to increase with increasing in-neck velocities. This nonlinear effect is a consequence of turbulence and jets forming at the interfaces between the neck and the inner cavity and the exterior environment, causing increased acoustic resistance. In many cases, the level dependence of the behavior can be partially overcome by increasing the cavity or neck damping by enhanced increased level-independent resistance of an incorporated porous material, which leads to lower in-neck velocity magnitudes, but leads to at least partial loss of the WDHR-specific reflection characteristics. A WDHR with level-independent reflection characteristics would be beneficial for narrow-band room acoustic corrections such as damping of modes or their redistribution over the spectrum. In this work, chamfering of the resonator neck edges is used as a strategy to obtain a weakly damped resonator with sound pressure level independent behavior.

Keywords: *Helmholtz resonator, perforated board, neck shape, chamfer, impedance tube*

**Corresponding author*: *David.Jun@vut.cz.*

1. INTRODUCTION

Helmholtz resonators (HRs) are devices that can be used for acoustic applications by utilizing a compressible cavity with an open aperture (neck) in order to achieve subwavelength resonance. A weakly damped Helmholtz resonator (WDHR) is a variant of an HR, having its surface resistance near resonance substantially lower than that of air so that the sound reflection at its resonance is out-of-phase. Such behavior can be exploited for selective mode damping or manipulation [1–3] or scattering [4]. WDHRs are generally known for their characteristics being dependent on the in-neck velocity, which is also part of the focus of this contribution.

Ingard and Labate [5] studied the formation of vortices and jets on perforated boards and modeled the structure by defining four distinct regimes of nonlinear behavior in terms of the average particle velocity in the orifice. In the first region, vortices start to form around the orifice edges; in the fourth one, the turbulent jet is fully developed at least at one side of the orifice. It is worth noting that the authors pointed out that at resonance "nonlinear effects become of importance for sound pressure levels of about 65 dB for the incoming wave". The occurrence of nonlinear effects at this moderate sound pressure level makes the phenomenon relevant also for room acoustics. A few years later, Ingard [6] published his major work on Helmholtz resonator design, covering also the non-linear behavior. Ingard here introduced the following term for resonator resistance using neck end correction lengths:

$$\rho_0 c_0 \theta_{\text{total}} = \rho c(\theta_{\text{l}} + \theta_{\text{nl}}) = \frac{2R_s}{r_0}\left(t + \Delta_{\text{l}} + \Delta_{\text{nl}}\right) \quad (1)$$

where $\rho_0 c_0$ is the characteristic specific impedance

of air, ρ_0 the density, and c_0 the speed of sound in air. The dimensionless correction θ_{total} [-] accounts for both the linear θ_{l} [-] and non-linear θ_{nl} [-] end correction effects related to the apparent neck length in terms of losses. The surface resistance R_s is given by $R_s = 0.5\sqrt{2\mu\rho\omega}$ [kg·m^{-1}·s^{-1}], where μ is the dynamic viscosity, r_0 is the neck radius, and t is the plate thickness. Δ_{l} and Δ_{nl} are the linear and non-linear end correction lengths for the neck length. According to his work, the linear end correction is given by $\Delta_{\text{l}} = 2r_0 = d$, and the non-linear end correction Δ_{nl} can be expressed for sufficiently thick plates using the empirical equation:

$$\frac{\Delta_{\text{nl}}}{d} = C u_0^n \tag{2}$$

where C and n are parameters that might show some frequency dependence and u_0 [m/s] is the particle velocity magnitude in the aperture. The work of Blackman [7], however, reported experimental results that aligned rather poorly with the above model. Later, Ingard and Ising [8] further refined his findings, showing that at high pressure levels (in the 4th regime), the resistance of the orifice is approximately given by

$$R \approx \rho_0 u_0 \tag{3}$$

Melling [9] further extended this relation by invoking the particle velocity-dependent "orifice discharge coefficient", C_D [-], as part of the proportionality factor between R and ru_0. The discharge coefficient was known from fluid dynamics and had been studied already in a steady-state situation with constant flow by Johansen and Southwell [10]. While Melling [9] was mainly interested in the highest nonlinear regime, where C_D asymptotically reaches a constant value, the earlier steady flow-focused work of Johansen and Southwell [10] showed the potential of this parameter to identify and describe also the remaining regimes. Despite that, no model has been proposed for these lower regimes by any of the authors mentioned above.

More recently, the non-linear behavior in the orifice was exploited in micro-perforated panels (MPP) and was characterized via a non-linear impedance [11–14]. Investigations of non-linear HR behavior (or more generally, perforated plates) are still ongoing, mainly at high sound pressure levels [15] or for measurement applications [16].

In room acoustics-related applications, sound pressure level (SPL)-dependent damping characteristics are typically not considered or generally unwanted, since the most common room acoustic measures rely on linear acoustics assumptions. The objective of the current work is to reduce nonlinearities by shifting the transition from the first most weakly nonlinear regime to the other ones towards higher SPL levels. This approach is followed by chamfering the neck edges.

2. METHODS

The insight on the effect of chamfering was gained by analyzing the in-neck velocity, the in-neck Reynolds number, and the incident pressure, which were extracted from impedance tube measurements. The two-microphone impedance tube method was used according to ISO 10534-2 [17]. In this method, the pressure reflection factor of the WDHR resonator, r, is retrieved from the transfer function measured between two microphone positions, $H_{12} = \frac{p_2}{p_1}$, where p_1 and p_2 are the acoustic pressures measured at the respective microphone positions. The surface acoustic impedance was then obtained from the pressure reflection coefficient via

$$Z_s = R + jX = \frac{1+r}{1-r} \cdot Z_0, \tag{4}$$

where R, the real part of Z_s, is the surface resistance, X is the surface reactance, and $Z_0 = \rho_0 c_0$ is the characteristic impedance of air. The impedance tube used in this study was a next-generation version of the one used and validated in [18]. The tube in this study was made out of steel and had a square cross-section. The lateral dimensions were 102×102 mm^2, the steel wall thickness was 4 mm, and the rigid termination was 30 mm deep. The tube corners were rounded with a radius of 4 mm. The tube frequency range, given by its geometry, was 40 Hz to 1680 Hz. The acquisition chain consisted of two Behringer ECM8000 microphones, a Focusrite Scarlett 18i20 Gen3 sound card, and a Fedora Linux-powered mini PC running Python-based "imptube" software [18]. On the sound source side, a logarithmic sweep was played through a t.amp S75 MKII power amplifier and a low to medium frequency range 6.5" loudspeaker with a working frequency range of 40 to 4500 Hz.

At first, in the analysis phase, the instantaneous sound pressure $p_{m,\text{norm}}(f)$ in the tube was obtained according to Figure 1. The input sweep $y_{\text{in}}(t)$ was normalized to the full-scale range of -1 to 1, and its spectrum was used as a reference $y_{\text{in,norm}}(f)$ for calculating the instantaneous values relative to full scale $y_{m,\text{norm}}(f)$.

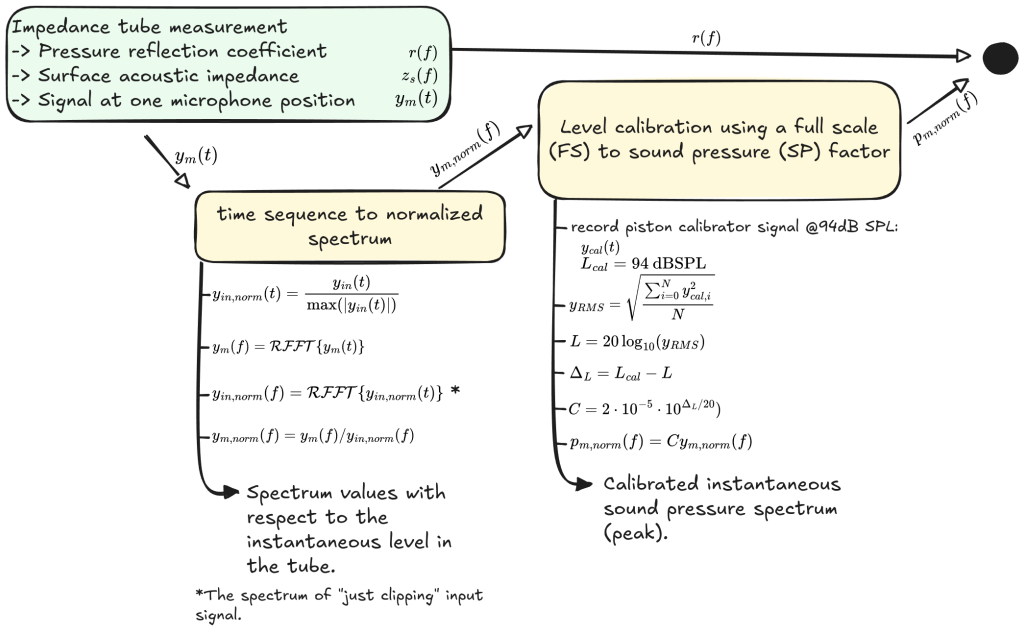

Figure 1. Procedure for obtaining the instantaneous sound pressure from an impedance tube measurement. The measured time sequence was first transformed to frequency domain and then divided by the "just-clipping" input sweep spectrum. That led to a spectrum expressing for each frequency its headroom towards clipping. Level calibration was based on a piston calibrator measurement, its RMS level and the subtraction of the calibrator level value (94 dB) and the recorded signal value. The latter was converted to a factor applied to the instantaneous pressure spectrum.

$$y_{m,\text{norm}}(f) = \frac{y_m(f)}{y_{\text{in,norm}}(f)} \tag{5}$$

This representation yields the spectrum with respect to the instantaneous level in the tube for each frequency bin. These values were converted to the physical pressure $p_{m,\text{norm}}(f)$ using a piston calibrator of known RMS SPL level.

Assuming plane wave propagation normal to the test specimen, the sound field can be decomposed into two opposing waves, and the homogeneous particle velocity can be obtained as a function of the acoustic pressure at a microphone position, $p(x_m)$, and the pressure reflection factor at the specimen surface r.

$$u(x=0) = \frac{p(x_m)\cdot(1-r)}{Z_0\left(e^{-jkx_m} + re^{jkx_m}\right)} \tag{6}$$

The average particle velocity in the neck of a plate perforation can be expressed as

$$u_0 = \frac{u(x=0)}{\phi} \tag{7}$$

where $\phi = \frac{A_n}{A}$ is the open plate porosity, i.e., the ratio between the neck cross-section surface A_0 and the total specimen surface A. The velocity can be used for calculating the in-neck Reynolds number Re:

$$\text{Re} = \frac{\rho_0 u_0 L}{\mu} \tag{8}$$

where L is the characteristic length (in this case, the perforation diameter d), $\mu = 1.84 \times 10^{-5}$ Pa·s is the dynamic viscosity of air, and u_0 is the particle velocity magnitude. Similarly, the in-neck displacement ξ [m] can be obtained:

$$\xi = \frac{u_0(f)}{i\omega} \tag{9}$$

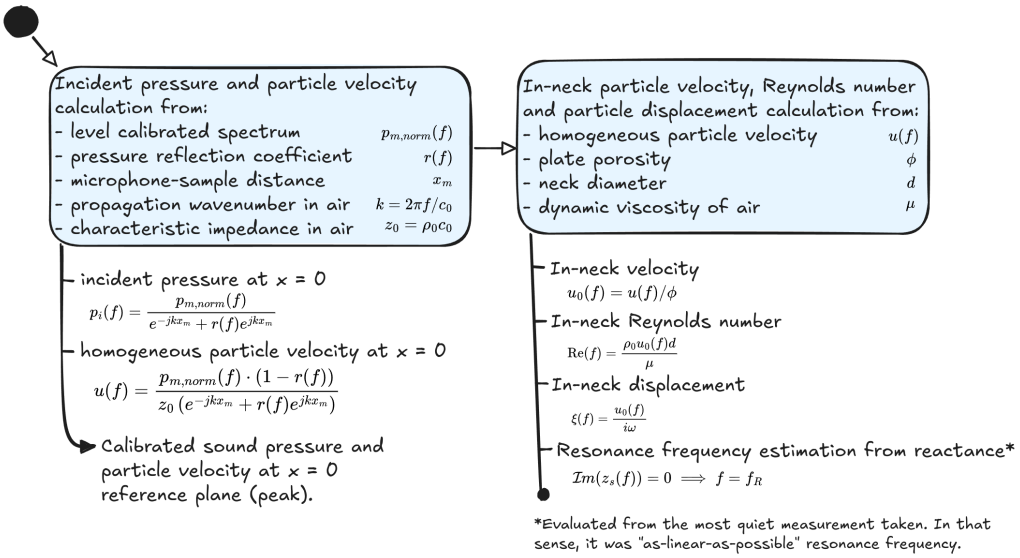

Figure 2. Calculation summary for the incident pressure, in-neck particle velocity, Reynolds number and displacement.

Similarly to the homogeneous velocity, also the incident pressure can be obtained from a plane wave reflection measurement as

$$p_i = \frac{p(x_m)}{e^{-jkx_m} + re^{jkx_m}}. \tag{10}$$

The calculation overview is shown in Figure 2.

3. RESULTS AND DISCUSSION

Two perforated plate variants were measured under different pressure levels in the tube. Both shared most of the geometrical parameters: the neck diameter $d = 12\,\mathrm{mm}$, the virtual neck spacing (the lateral dimension of the tube) $D = 102\,\mathrm{mm}$, the plate thickness $t = 9\,\mathrm{mm}$, and the cavity depth behind the plate $d_c = 200\,\mathrm{mm}$. The only changing parameter was the presence/absence of a 1 mm deep chamfer cut at 45° from both sides of the neck.

In the following, the quantities are presented only at the resonance frequency obtained from the acoustic reactance of the most quiet measurement. In that sense, it was the as-linear-as-possible resonant frequency obtained through measurements. This choice was done for two reasons, which appeared during the analysis: (a) At the resonance frequency, HRs show a rather simple behavior of either completely in- or out-of-phase response, leading to a pressure maximum or minimum directly in the neck. (b) The response at the resonance frequency seems to drive also the response in its vicinity. More precisely, a similar degree of nonlinearity is observed near the resonance, even though the calculated in-neck velocities differ.

Figure 3 shows the normal incidence absorption coefficient with respect to the incident pressure level. In both cases, the values started at about 0.5 for lower levels, reach a maximum, and start to decrease again. The decrease happens when the acoustic resistance crosses the characteristic impedance of air. Maximum absorption is reached for both cases at different levels, which are approximately 3.5 dB apart in incident SPL. The average difference for $0.5 < \alpha < 0.9$ between the two cases is $\Delta L_p = 10.6 \pm 3.2\,\mathrm{dB}$. Since the analysis does not account for the resonance frequency shift at high levels, the chamfered variant does not reach the $\alpha = 1$ point.

Figure 4 puts the findings in the context of in-neck velocity and Reynolds number. These results can be qualitatively compared to the previous studies. Johansen and Southwell [10] reported for low porosity plates that the transition between the weakly velocity-dependent regime 1 and the strongly velocity-dependent regime 4 happens at $10 < \sqrt{\mathrm{Re}_0} < 40$, which seems to align rather well with the presented results. For the chamfered variant, this transition is shifted towards higher Reynolds num-

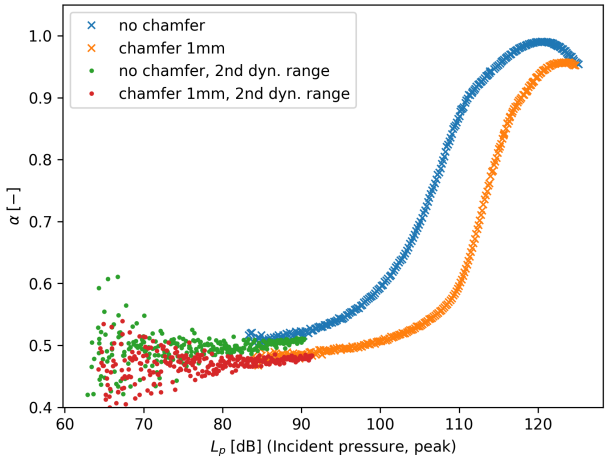

Figure 3. Normal incidence absorption coefficient at the resonance frequency as a function of incident SPL level (peak). Two dynamic ranges of measurements were tested for both orifice variants. In the first one (blue and orange), there is a minor offset between the levels of approx. 0.2 dB, in the second one 0.1 dB (green and red).

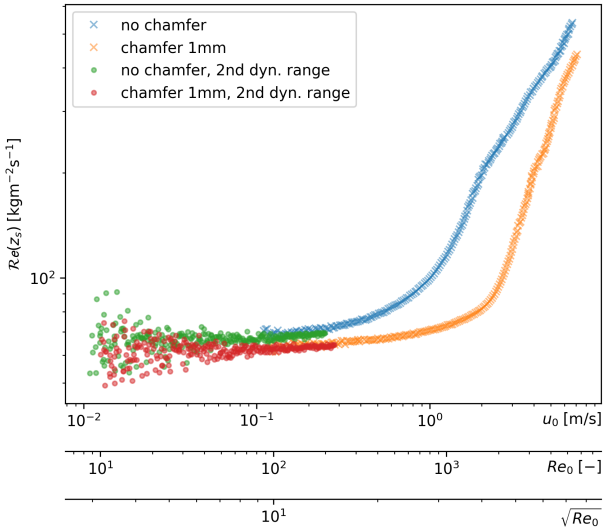

Figure 4. Normal incidence surface resistance as a function of in-neck velocity amplitude, Reynolds number and its square root. Two dynamic ranges of measurements were tested for both orifice variants. In the first one (blue and orange), input sweep level spacing is approx. 0.2 dB, in the second one 0.1 dB (green and red).

bers. When comparing to Ingard and Labate [5], we need to extrapolate their findings. At 224 Hz and for a plate thickness of 9 mm, they located the transition between $0.5 < u_0 < 2$ m/s. Based on their experiments and assumptions, both values of this range should decrease towards lower frequencies. In the present case, the transition roughly happens in the range originally assigned to $f = 224$ Hz.

It is important to note that it is not feasible to strictly connect the definitions of the different regimes between different authors, such as Ingard and Labate, Johansen, or Melling. For Labate and Ingard, regime 4 started when the turbulent jet appears at least on one side of the plate. In the view of Johansen's and Melling's discussions, no strict transition boundaries were mentioned, but a full turbulent jet was assumed as the limit at which the discharge coefficient stabilizes and which could be seen as the boundary of the final regime.

4. CONCLUSIONS

The objective of this study was to extend the weakly non-linear regime of a Helmholtz resonator reflection response towards higher incident sound pressures. The effect of neck chamfering was studied under normal incidence conditions in an impedance tube. The instantaneous sound pressure amplitude was used to calculate the in-neck velocity and the Reynolds number in order to allow for a more in-depth view of the problem. The results for the sharp-edge variant were found to be in good qualitative agreement with previous studies [5, 6, 10]. The chamfered variant showed an uplift of $\Delta L_p = 10.6 \pm 3.2$ dB in terms of the level difference at which the transition to more strongly non-linear regimes happens.

Future research should focus on a more parameter-rich and in-depth description of the different non-linear regimes as well as on the neck shape influence on them. For the sake of comparison, steady flow measurements should be conducted in a flow resistivity setup to further verify the discharge coefficients obtained acoustically and under steady flow.

5. ACKNOWLEDGMENTS

This project has received funding from the European Union's Horizon Europe research & innovation programme under the HORIZON-MSCA-2021-DN-01 grant agreement No. 101072598 – "ActaReBuild". The contribution was produced also with support for specific university research at Brno University of Technology, FAST-S-24-8572 and FAST-S-25-8768.

6. REFERENCES

[1] F. J. Fahy and C. Schofield, "A note on the interaction between a Helmholtz resonator and an acoustic mode of an enclosure," *Journal of Sound and Vibration*, vol. 72, pp. 365–378, Oct. 1980.

[2] J. Klaus, I. Bork, M. Graf, and G. P. Ostermeyer, "On the adjustment of Helmholtz resonators," *Applied Acoustics*, vol. 77, pp. 37–41, 2014.

[3] D. Jun, J. Plasek, M. Rychtarikova, and C. Glorieux, "Room modes in rectangular rooms with complex impedance boundaries," in *Juniorstav 2024: Proceedings 26th International Scientific Conference Of Civil Engineering*, (Brno, Czech republic), p. 8, Brno University of Technology, 2024.

[4] N. Jiménez, T. Cox, V. Romero-García, and J.-P. Groby, "Metadiffusers: Deep-subwavelength sound diffusers," *Scientific Reports*, vol. 7, Dec. 2017.

[5] U. Ingard and S. Labate, "Acoustic Circulation Effects and the Nonlinear Impedance of Orifices," *The Journal of the Acoustical Society of America*, vol. 22, pp. 211–218, Mar. 1950.

[6] U. Ingard, "On the theory and design of acoustic resonators," *Journal of the Acoustical Society of America*, vol. 25, no. 6, pp. 1037–1061, 1953.

[7] A. W. Blackman, "Effect of Nonlinear Losses on the Design of Absorbers for Combustion Instabilities," *ARS Journal*, vol. 30, pp. 1022–1028, Nov. 1960.

[8] U. Ingard and H. Ising, "Acoustic Nonlinearity of an Orifice," *The Journal of the Acoustical Society of America*, vol. 42, pp. 6–17, July 1967.

[9] T. H. Melling, "The acoustic impendance of perforates at medium and high sound pressure levels," *Journal of Sound and Vibration*, vol. 29, pp. 1–65, July 1973.

[10] F. C. Johansen and R. V. Southwell, "Flow through pipe orifices at low Reynolds numbers," *Proceedings of the Royal Society of London. Series A, Containing Papers of a Mathematical and Physical Character*, vol. 126, pp. 231–245, Jan. 1930.

[11] D.-Y. Maa, "Microperforated panel at high sound intensity," in *Proceedings of Inter Noise 94*, (Yokohama, Japan), pp. 1511–1514, 1994.

[12] D.-Y. Maa, "Potential of microperforated panel absorber," *The Journal of the Acoustical Society of America*, vol. 104, pp. 2861–2866, Nov. 1998.

[13] S.-H. Park, "A design method of micro-perforated panel absorber at high sound pressure environment in launcher fairings," *Journal of Sound and Vibration*, vol. 332, pp. 521–535, Feb. 2013.

[14] Z. Laly, N. Atalla, and S.-A. Meslioui, "Acoustical modeling of micro-perforated panel at high sound pressure levels using equivalent fluid approach," *Journal of Sound and Vibration*, vol. 427, pp. 134–158, Aug. 2018.

[15] A. Komkin, A. Bykov, and M. Mironov, "Experimental study of nonlinear acoustic impedance of circular orifices," *The Journal of the Acoustical Society of America*, vol. 148, pp. 1391–1403, Sept. 2020.

[16] E. Di Giulio, R. Di Leva, and R. Dragonetti, "Theoretical and Experimental Assessment of Nonlinear Acoustic Effects through an Orifice," *Acoustics*, vol. 6, pp. 818–833, Dec. 2024.

[17] "ISO 10534-2:1998, Acoustics-Determination of sound absorption coefficient and impedance in impedance tubes-Part 2: Transfer-function method," 1998.

[18] D. Jun and J. Plasek, "Impedance Tube Solution for Helmholtz Resonator Prototyping," *Acoustics Australia*, Jan. 2025.